Comprehensive Energy Analysis Report

University of Colorado
Solar Decathlon 2007

Comprehensive Energy Analysis Report

Submitted to

Michael Wassmer
National Renewable Energy Laboratory
Mail Stop 3214
1617 Cole Blvd.
Golden, CO 80401

Prepared by

University of Colorado Solar Decathlon Team

Contact Information

Solar Decathlon
University of Colorado
Civil, Environmental, and Architectural Engineering
428 UCB, Room ECCE 441,
Boulder, CO 80309-0428
303.492.6382
303.492.7317 fax
solar.decathlon@colorado.edu
http://solar.colorado.edu

7 August 2007

CONTENTS

INFLUENCE OF ENERGY ANALYSIS ON HOUSE DESIGN AND COMPETITION STRATEGY 2

Introduction 2

System Description 3

Loads Analysis 5

HVAC System 9

Architecturally Integrated Heat Exchangers 10

Building Integrated Photovoltaic/Thermal System 12

Natural Ventilation 15

Lighting 16

PROJECTED PERFORMANCE OF COMPLETE HOUSE DESIGN ON AN ANNUAL BASIS 19

Modeling Approach 19

TRNSYS Model Definition 20

Case Descriptions 22

Results 23

Conclusions 28

INFLUENCE OF ENERGY ANALYSIS ON HOUSE DESIGN AND COMPETITION STRATEGY

In order to achieve superior energy performance for the Solar Decathlon house, architectural and engineering design have been closely integrated and informed by one another. This is evident in decisions regarding the placement and size of windows, daylighting and electric lighting choices, natural ventilation, photovoltaic panels, and various system components. The house design has thusly been significantly modified since the completion of the schematic energy analysis report, which required the development of a new energy model and more detailed analysis. These analyses are described in the following sections.

Introduction

The CU Solar Decathlon house employs a number of novel systems that are difficult to model using standard simulation tools. The envelope modeling is straightforward enough to use Energy+. The systems, however, are too complicated to be modeled in Energy+.

A summary of the modeling tools used is shown in Table 1.

Table 1: Modeling tools used

	Modeling tool	
Category	**Conceptual**	**Comprehensive**
Building Envelope	Energy-10	Energy+
Photovoltaics	PV-Fchart	TRNSYS
PV/Thermal		MATLAB/PHOENICS/TRNSYS
Natural ventilation	PHOENICS	PHOENICS
Heat exchanger performance		PHOENICS
Systems	Excel	MATLAB/TRNSYS
Controls	Excel	MATLAB/TRNSYS
Electric Lighting	Excel	AGI32
Daylighting		AGI32

Energy+ calculates surface temperatures accurately and tracks the temperature and humidity of passively conditioned spaces. While the currently available version may have some gaps, Energy+ allows for an accurate model of the envelope and calculate zone thermal loads. Most building operating assumptions were borrowed from the Building America Benchmark. Energy+ was used to optimize the windows and design the sunspace. Hourly output could be analyzed to meet thermal comfort requirements.

PHOENICS uses surface temperatures to develop room airflow and temperature models. Surface temperatures can be captured from Energy+ for design day conditions. In addition, PHOENICS can be used to determine a building exterior pressure distribution for use in designing natural ventilation systems for passive cooling. These exterior pressures can then be applied to a building interior CFD model in PHOENICS to determine airflow and temperature distribution during periods of natural ventilation.

After loads are derived from Energy+, they can be used to drive a systems model. The initial model of the heat pump and storage system was constructed in Excel. The Excel model only allowed simple setpoint controls to be implemented. More advanced controls work was conducted using MATLAB and then TRNSYS to model the systems, including interaction with the PV/T system.

Early lighting system design was conducted using a Lumen Method spreadsheet analysis in Excel. This allowed for a rough estimate of the lighting requirements of each space. Further analysis was conducted in AGI32 to more accurately calculate the illuminance on certain surfaces and the amount of interreflected light within the space. Additionally, daylighting analysis was conducted in AGI32, by modeling crucial spaces within the Solar Decathlon house at certain times of day throughout the year.

System Description

The University of Colorado Solar Decathlon home is unique in several respects. One important distinction between this year's CU entry and previous years' entries is the decision to design and construct a net-zero energy home the size of a typical American home. Although the house we bring to the National Mall will be under the 800ft^2 footprint limit, it will contain all of the systems required to operate the entire 2100ft^2 house.

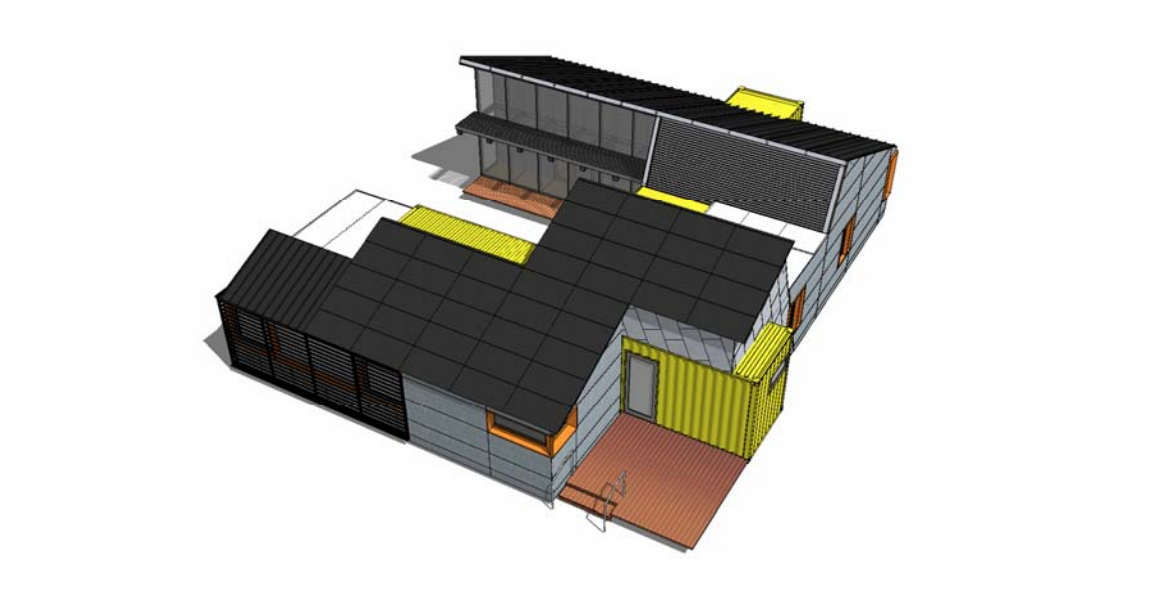

Figure 1: University of Colorado Solar Decathlon complete house rendering

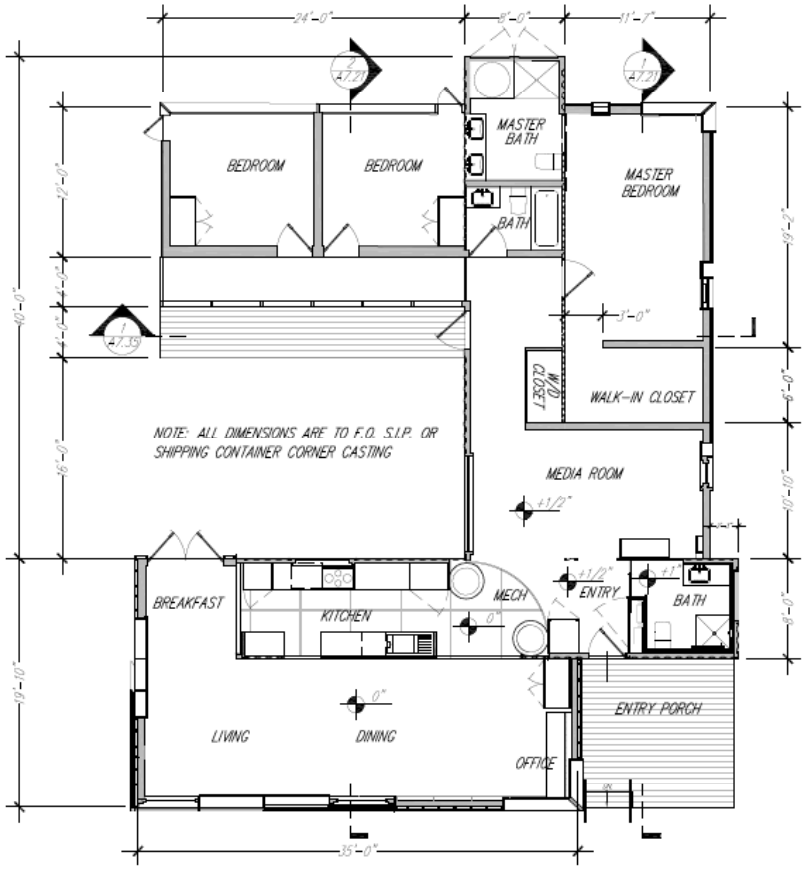

Figure 2: University of Colorado Solar Decathlon complete house floor plan

The HVAC system is a hydronic system composed of a water-to-water heat pump coupled to two thermal storage tanks. The heat pump maintains a setpoint temperature in either the hot or cold tank depending on the need for heating or cooling. A dedicated domestic hot water mode on the heat pump creates hot water for domestic use.

The photovoltaic system will be fully integrated into the roof surface, eliminating the need for a traditional roofing material. The framing system used allows the PV panels to be turned into large shingles mounted less than 3 inches from the roof deck. Behind the PV is a custom designed and fabricated photovoltaic thermal system (PV/T). The system will offset efficiency losses due to increased cell temperatures resulting from un-ventilated roof integrated PV. The PV/T simultaneously cools the PV, making it more efficient, and capturing waste heat to satisfy building loads. The PV/T system connects to both tanks, allowing heat to be collected from the PV during the winter for space heating, and rejected at night through the roof during the summer.

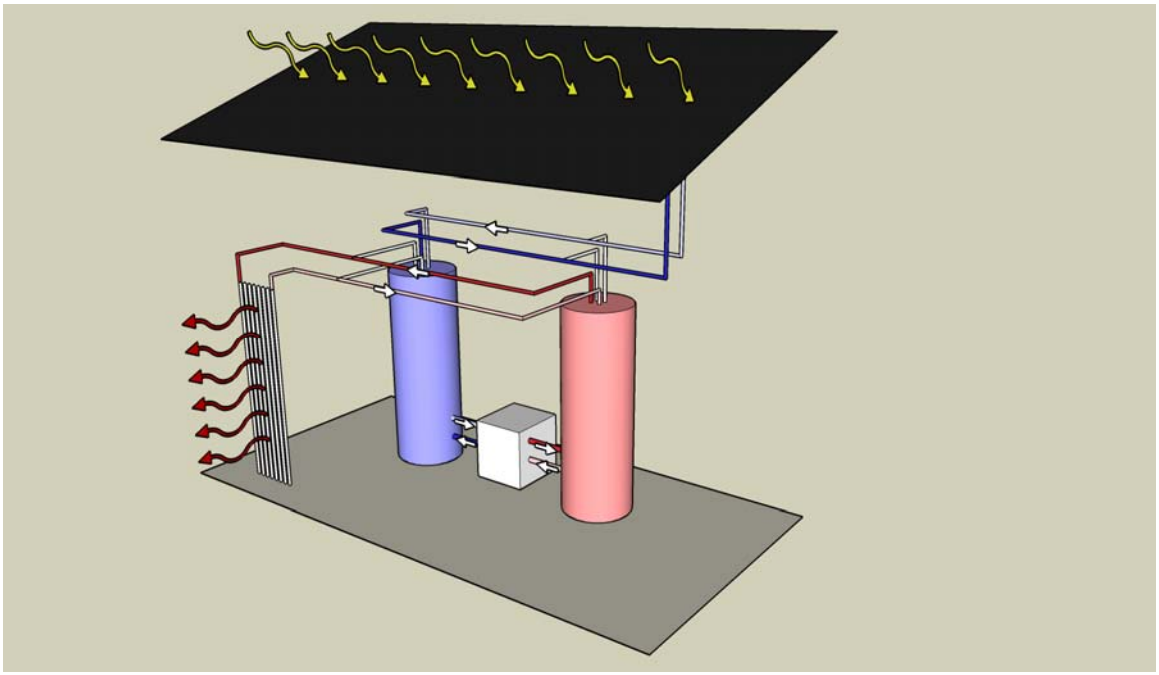

Figure 3: Typical cold weather operation of HVAC and BIPV/T system

Outdoor heat exchangers supplement the PV/T and reject heat to the outdoors when the hot tank becomes too hot and heat rejection is not possible through the roof. Under certain conditions, the outdoor heat exchanger can be used to heat the cold tank when the PV/T system is not capable of doing so.

Custom-built radiant/convective heat exchangers within the building connect to the two storage tanks to satisfy building loads. These heat exchangers are not modeled in the simulation.

Loads Analysis

An Energy+ model of the house was developed in order to analyze heating and cooling loads, and to inform decisions regarding the building envelope. The house was divided into four zones – south, east, north, and sunspace – shown in Figure 4.

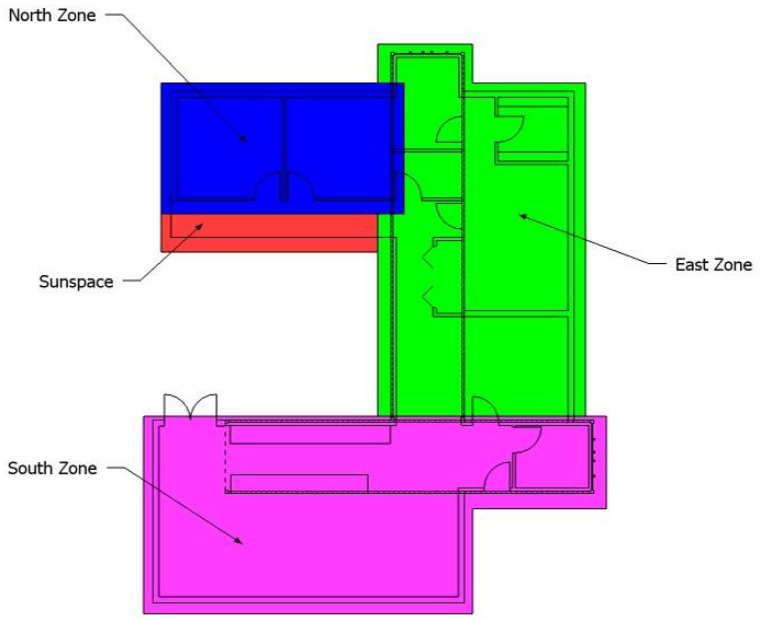

Figure 4: Zones in EnergyPlus model

Windows

The size, type, and location of windows can have a large impact upon energy performance. Windows are also an important architectural element, so decisions were made with architectural considerations in mind. Figure 5 shows a comparison of heating and cooling loads for different glazing types.

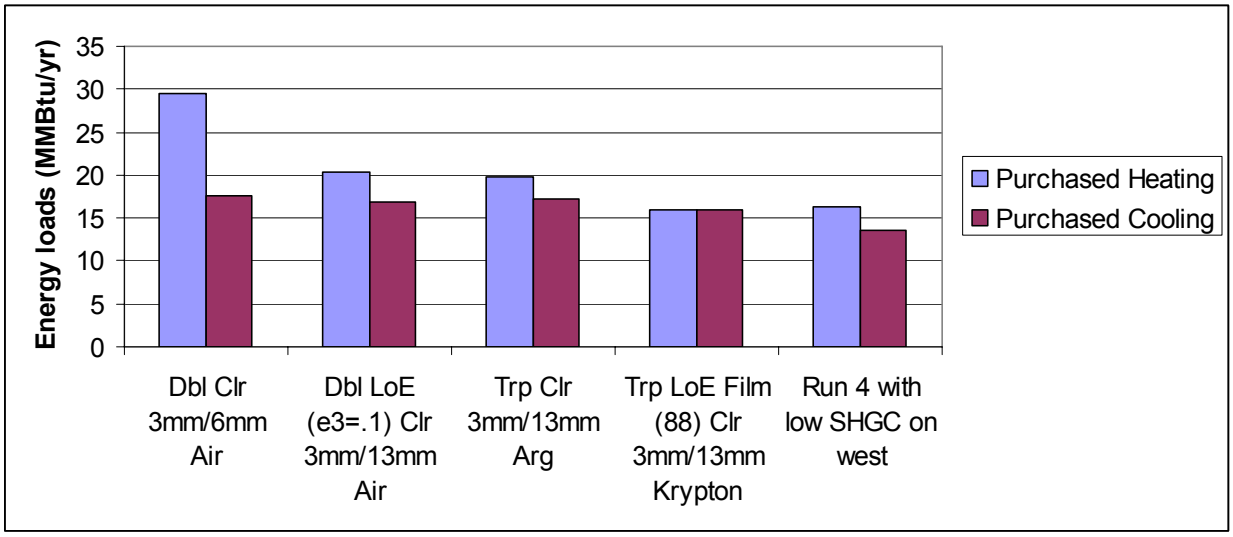

Figure 5: Glazing type parametrics

Five different glazing types were investigated. The last run examined the use of windows with a lower solar heat gain coefficient on the west façade only. Heating loads increased slightly, but the cooling load decreased substantially. These results can be seen in Figure 6.

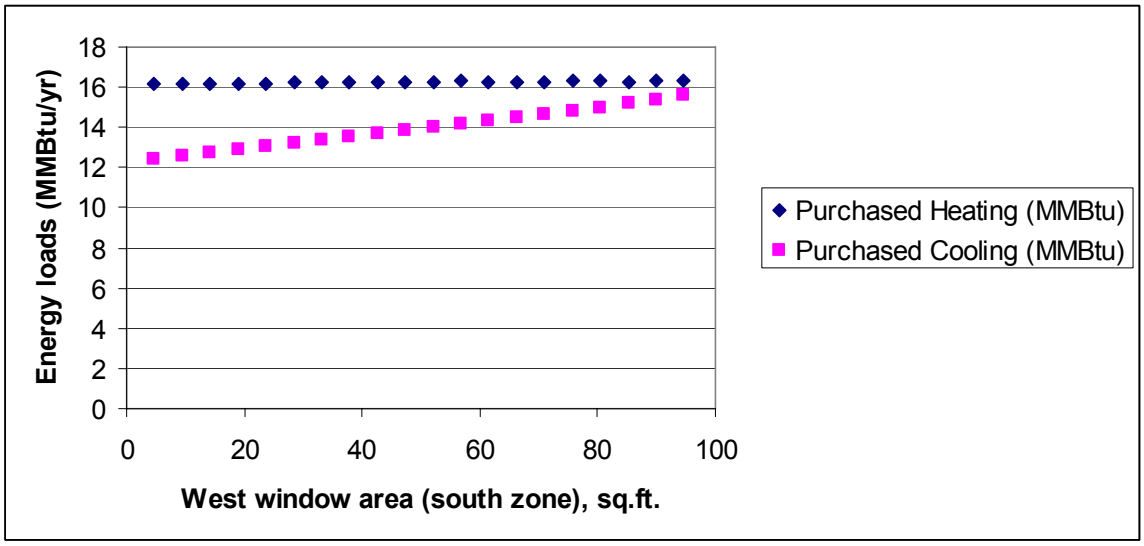

Figure 6: West-facing glazing area analysis

The west-facing window in the south zone presented a challenge for both the architectural and engineering teams. The architects required a large glazing area to maximize mountain views to the west, while the engineers wanted a small window area to minimize cooling loads. As with many facets of the engineer/architect relationship, this part of the decision making process comprised a negotiation, rather than an optimization.

Sunspace

Energy+ was similarly used to determine the heating and cooling loads and interior conditions within the sunspace. Table 1-2 displays the relationship between south façade glazing in the sunspace and its heating and cooling loads.

Table 2: Sunspace glazing type and area

	Glazing	South Glazing area (m^2)	West Glazing area (m^2)	Cooling (MMBtu)	Heating (MMBtu)
A	Dbl LoE (e3=.1) Clr 3mm/13mm Air	18	2.75	9.6	25.6
B	Dbl LoE (e3=.1) Clr 3mm/13mm Air	21.6	3.3	9.7	25.3
C	Dbl LoE (e3=.1) Clr 3mm/13mm Air	14.4	2.2	9.5	25.4
D	Dbl Clear	18	2.75	9.5	26.5

The hourly output in Figure 7 shows the interior thermal comfort differences between Double Low-E and Double Clear glazing choices.

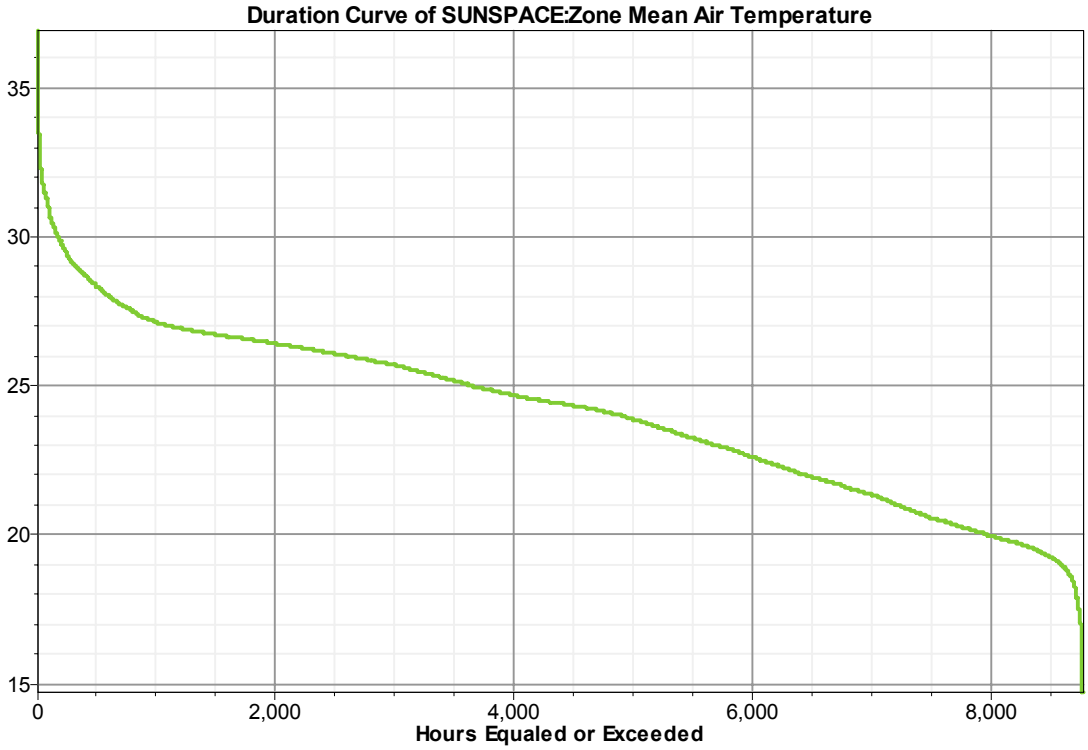

Figure 7: Sunspace temperature with Double Low-E glazing

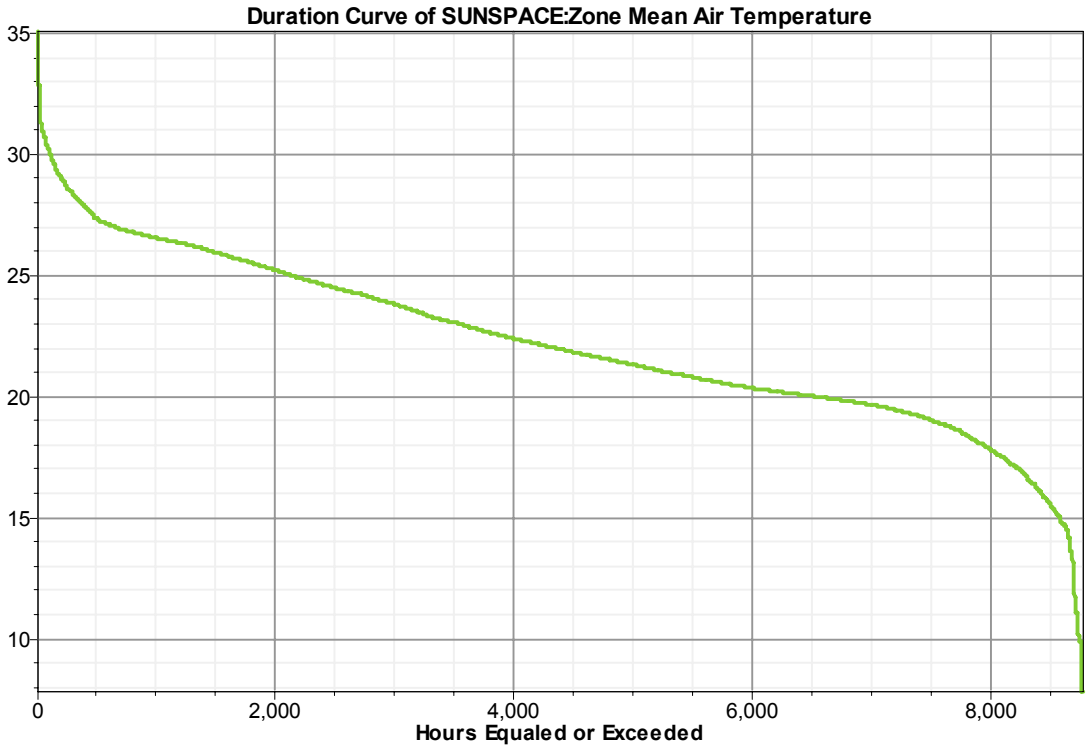

Figure 8: Sunspace temperature with Double Clear glazing

As seen in Figure 8, double Clear glazing does not meet the temperature requirements for unconditioned spaces.

HVAC System

Several important components of the HVAC system, the thermal storage system and water-to-water heat pump were modeled using Excel. The system nominally contains a hot tank, a cold tank, a heat pump, and an outdoor heat exchanger. In general, the tanks allow storage of night cooling in the summer and day warming during the winter. A parametric study of annual energy use as a function of the tank temperatures was conducted.

Model Details

The model started with hourly loads from an Energy+ model of an iteration of the Solar Decathlon house, taking into account ambient temperature conditions. The two adiabatic tanks are controlled based on monthly setpoints for their minimum and maximum temperatures. The cold tank is modeled with ice storage available – this is used during the heating season. A water to water heat pump with manufacturer's performance data from WaterFurnace™ connects the two tanks. When it is necessary to cool the cold tank or heat the hot tank, the heat pump does this work and the energy use is calculated. When it is desirable to dump or collect heat from outside, the model uses a simple UA model of an outdoor heat exchanger. Note, however, that this only happens with a desirable temperature difference of 5 degrees F or more. The heat pump does not meet the heating load by itself in all conditions, if the storage is small. This occurs when the cold side temperature gets too low, since the capacity of the heat pump drops rapidly with dropping low side temperatures. Under these high heating load conditions, electric resistance heating makes up the rest. The size of the storage has some impact then on the size of the heat pump necessary, but this aspect was not explored further.

Parametric Study and Results

The nominal UA-value for the outdoor heat exchanger is 1000 Btu/deg F-hr. The nominal tank sizes are 500 gallons of ice and 100 gallons of water on the cold side and 500 gallons of hot water on the warm side. With a nominal hot side heating temperature of 95 F and a cold side cooling temperature of 35 F, the system with storage uses 1800 kWh per year, vs. 2850 kWh per year for the system without storage. Figure 9 shows how the system temperatures vary through the year. The most striking aspect of the graph shows how the ice storage keeps the low side tank temperature at 32 degrees F for much of the winter with these tank sizes.

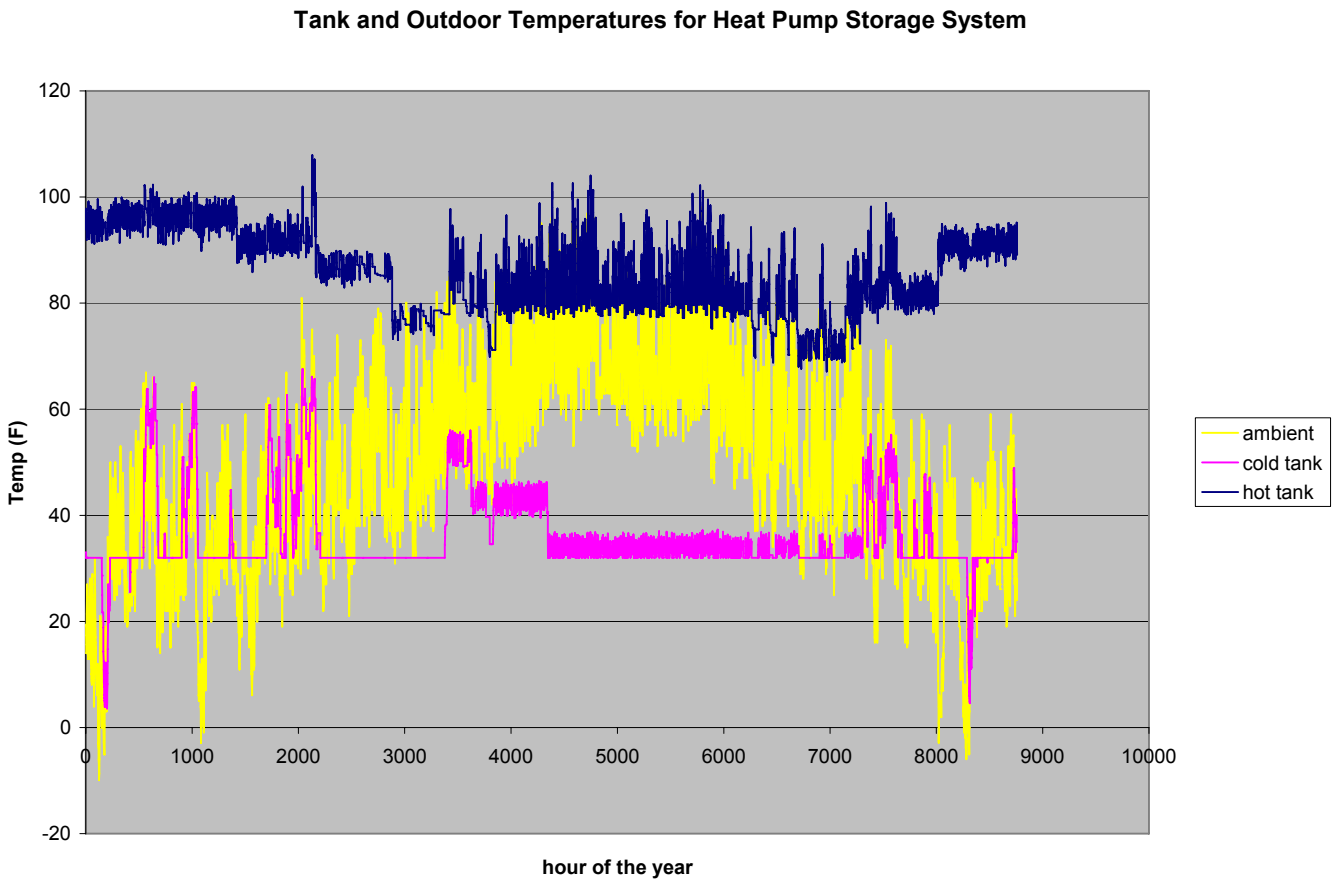

Figure 9: Temperatures of active thermal storage system

Architecturally Integrated Heat Exchangers

The design of low energy building HVAC systems requires a balance between energy efficiency methods and providing a suitable indoor environment for occupants. The Solar Decathlon house uses architecturally integrated (hybrid forced air / radiant) heat exchangers to condition the space. The heat exchangers consist of 2m tall bundles of copper pipes in a 2-row staggered arrangement. Values for approximate heat transfer characteristics were determined analytically based on calculations for tube bundles. The heat exchangers utilize heating hot water and chilled water from a heat pump/thermal storage system to supply heating and cooling to the space. The system utilizes both the radiant effect of the heat exchangers, forced convection, and buoyancy driven flow along the tubes for heat transfer.

Computational fluid dynamics (CFD) analysis was used to predict the comfort parameters for determining the predicted mean vote (PMV), mean age of air, and draught in the room. A sample PMV analysis can be seen in Figure 10.

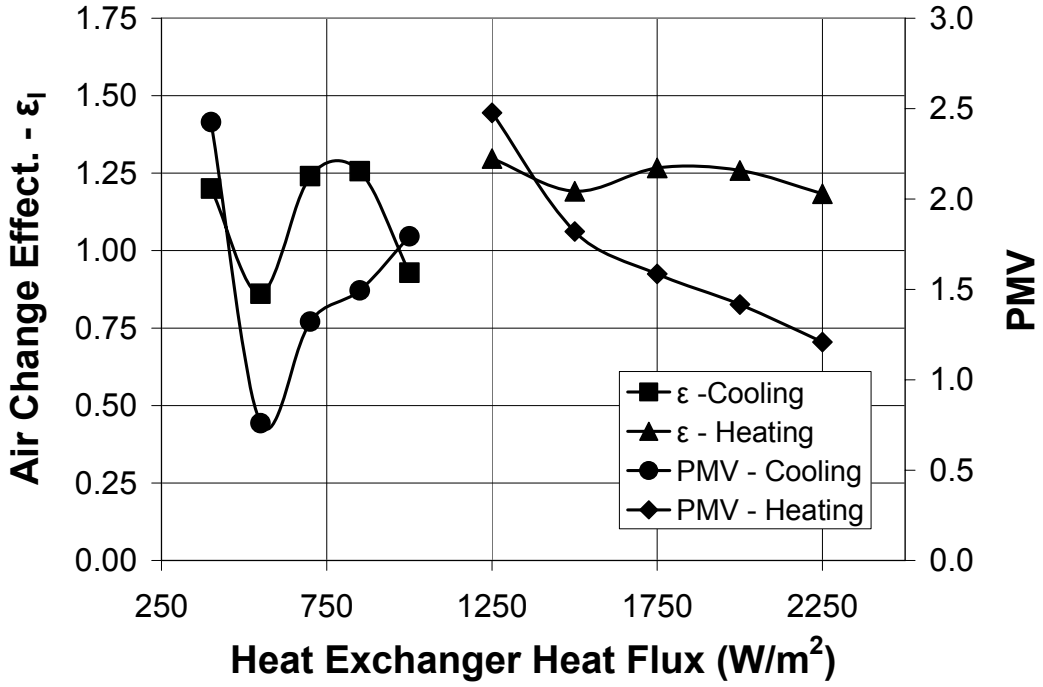

Figure 10: Predicted Mean Vote results for different air flow rates

The variables that are required to compute these comfort parameters are: air temperature, radiant temperature, air velocity, turbulence, clothing insulation, metabolic rate, and air density. Clothing levels of 0.5 for summer and 1.0 for winter were used per the ASHRAE Standard 55 recommendations. Figure 11 shows the results of PHOENICS model displaying air velocity within the space during cooling mode.

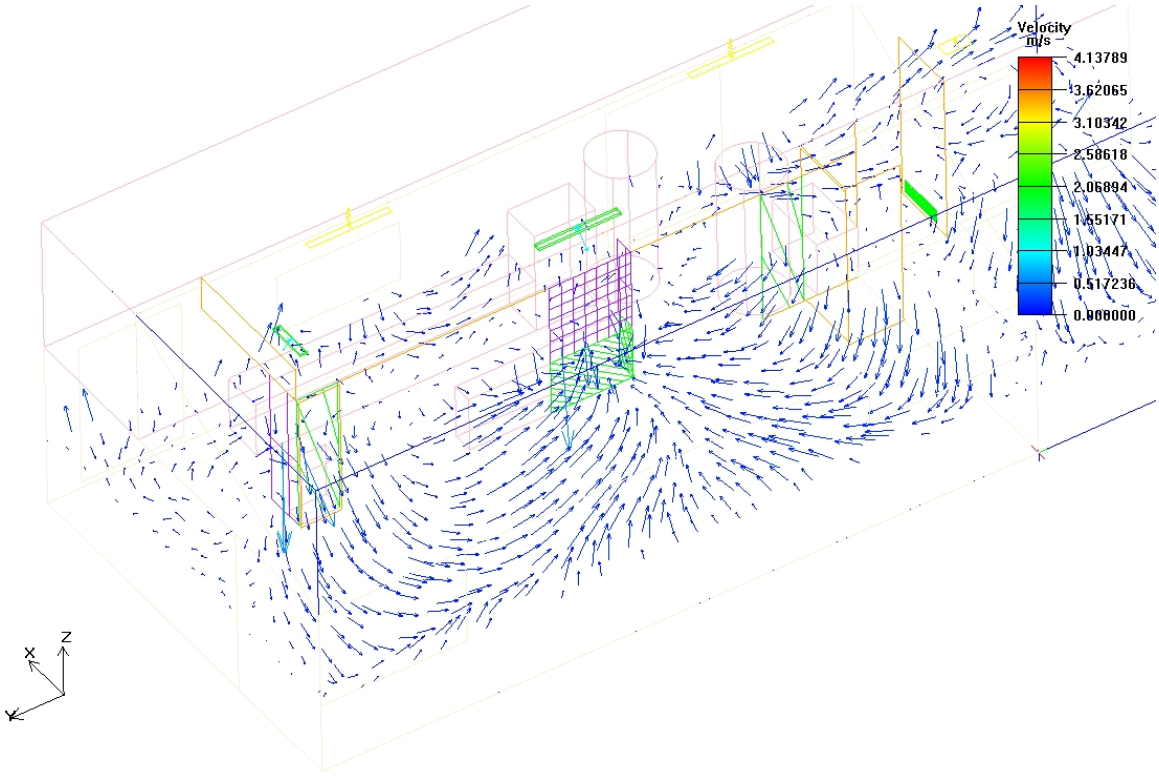

Figure 11: Free convection-driven air flow during cooling mode

Building Integrated Photovoltaic/Thermal System

The Solar Decathlon house will use combined photovoltaic-thermal collectors (PV/T) integrated into the building façade (BIPV/T), which promises to increase electrical efficiency and provide significant fractions of domestic hot water loads. The modeling algorithm developed combines a solar insolation processor, PV system model and heat transfer network to model the electrical and thermal performance of a water-cooled BIPV/T collector. The computer model was constructed in MATLAB and uses iterative techniques to solve the coupled, non-linear convective and radiative heat transfer coefficients and resulting energy balance between the environment and the collector components. Simulations were performed for an entire year using hourly weather data for Denver, Colorado. In all simulations, transient effects were ignored and collector components were assumed to be massless. Additionally, edge effects were neglected and the surface behind the collector was assumed to be adiabatic. Four different cases were examined. These were:

1. ***No heat recovery***: The base case for this study assumes that there is no heat recovery from the back of the panel. All steady-state heat transfer is accounted for by the convective and radiative losses to the ambient air and sky. This case approximates the typical building integrated application where natural convection and radiation only act upon the front surface of the PV module. This case represents the worst-case scenario against which improvements in cell efficiency and power output can be compared in subsequent cases. The simulation results show that the nonventilated BIPV collector is capable of producing 9,647 kWh of electricity over the course of the year. The predicted cell temperatures result in an average solar cell efficiency of 20.4%.

2. ***Constant collector inlet temperature***: In this case, a constant collector inlet temperature is chosen that approximates the mains temperature (10ºC). Water at this temperature is continuously circulated behind the PV module to remove heat from the cavity. Basic controls are implemented that limit circulation to times when heat can be removed, ie. when the water does not add additional heat to the cavity. This simulation allows for a direct electrical efficiency and power output comparison against the base case. Overall annual energy production for this system is predicted to be 10,088 kWh, 4.6% higher than the base case. Overall energy recovered from the back of the PV modules is predicted to be 25,358 kWh.
3. ***Typical domestic hot water load schedule***: This case simulates the performance of the collector in a stand-alone DHW system. The amount of useful energy collected goes to pre-heat the domestic hot water supply. Mains temperature water is used to make up the volume removed by the load and the tank temperature is allowed to float at any temperature below 80ºC. The same control system implemented in Case 2 is used in this simulation. Annual electrical efficiency and output are compared against the base case. Annual electrical yield falls to 9,528 kWh, with an overall cell efficiency of 19.7%. This reduction represents a 1.2% decrease in electrical output. Similarly, annual thermal yield falls to 13,716 kWh. This can be attributed to the higher inlet temperatures resulting from elevated storage tank temperatures. At higher inlet temperatures, less useful heating energy can be captured and the controls turn off circulation.
4. ***BIPV/T as an outdoor heat exchanger***: The ability of the collector to reject heat from a hot water storage tank is investigated as a means to cool water for space conditioning the next day. This simulation runs only at night. The tank is assumed to have the same volume, surface area and loss coefficient as that used in Case 3. The temperature is set to 60ºC at the beginning of each evening and is allowed to drop throughout the night. Total heat losses through the collector on an hourly basis for the entire year are predicted to be 24,017 kWh. Investigation of the computed overall heat loss coefficient, UL, for each hour of the year, results in an average value of 5.8 W/m2-K.

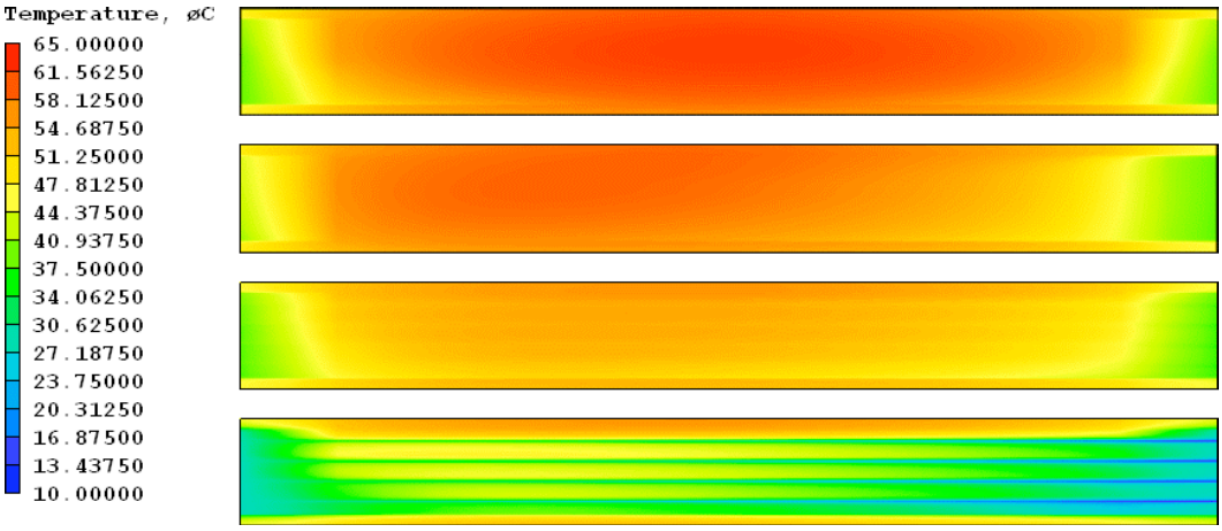

Figure 12: PV temperature contours for natural convection (top), forced convection (first from top), heat recovery (second from top), and temperature contour for absorber plate (bottom)

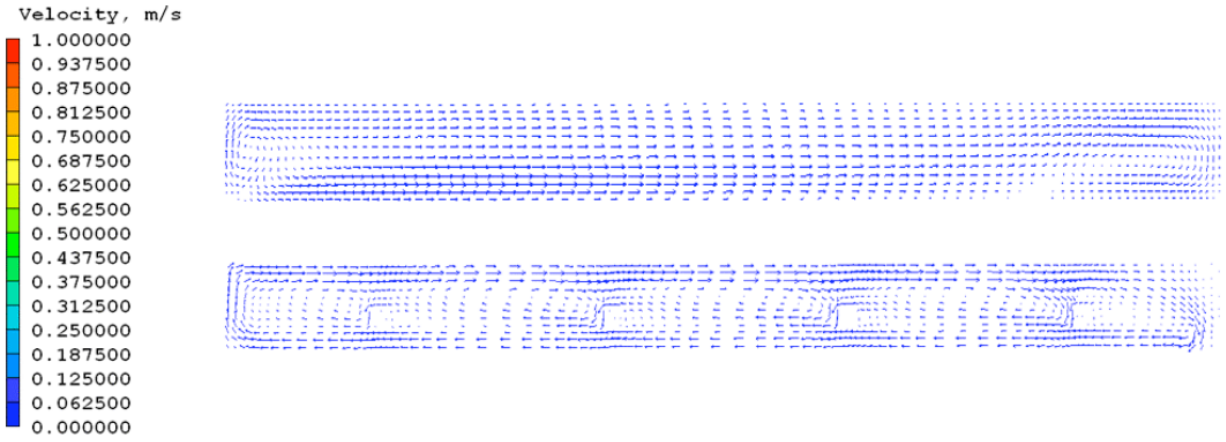

Figure 13: Velocity vectors in the cavity below the PV cells for natural convection (top) and heat recovery (bottom)

A second study of the BIPV/T collector was conducted in PHOENICS to examine temperature and velocity profiles of the collector under differing conditions. Temperature values at the bottom surface of the glass blockage were obtained by exporting the temperature contour as a comma separated text file. The bottom surface was chosen because the silicon cells composing the PV module are mounted there. It was assumed that the bottom surface temperature best approximates the silicon cell temperature. Similarly, exiting fluid temperatures for cases simulating heat recovery were also exported. Figure 12 shows temperature contours on the bottom surface for natural convection, forced convection and heat recovery. Insolation is 1000W/m^2 and inlet fluid temperature is 10ºC for the heat recovery case. The highest temperatures are seen in the natural convection case. The forced convection case shows slightly lower temperatures, but the heat recovery case shows the lowest. The local influence of the absorber channels on both the absorber plate and the PV cells can be clearly seen. Figure 13 illustrates the effect of the absorber plate on the airflow behind the PV cells. The section shown here is taken at the midpoint of the array, 3.65m from the east edge. Although the absolute value of the velocities are equivalent, the pattern of the flow is much more complex around the absorber plate. The outlines of each channel are clearly visible as are the five small convection loops that form above the absorber surface. In contrast, the natural ventilation case shows one large convection loop. The formation of small convection loops is a result of increased turbulence, which increases heat transfer between the back surface and the absorber plates. Maximum and average PV cell surface values are calculated from the exported data for comparison.

The study found that forced convection is capable of lowering cell temperatures a marginal amount relative to the natural convection case. Interestingly, water entering at 50ºC, hot enough for domestic hot water use, is capable of lowering cell temperatures over the forced convection case. Heat recovery is capable of lowering both average and maximum cell temperatures compared to both natural and forced convection. A 10ºC absorber inlet water temperature results in cell temperatures 5ºC lower than natural convection on average, and 10ºC lower at a maximum. Taking 10ºC as the water inlet temperature, a standard silicon cell with a temperature coefficient of 0.4%/ºC at an average of 5ºC reduction in temperature results in a 2% increase in conversion efficiency. Those cells operating at the maximum temperature see a 4.0% increase in conversion efficiency. Although gains in electrical output are modest for this collector, the amount of heat collected by active heat recovery can be significant. Outlet temperatures, averaged from the exported temperature contours are able to reach 55ºC, suitable for domestic use or for hydronic heating systems.

The proposed heat recovery method explored in this BIPV/T collector shows good potential for reducing PV cell temperatures and subsequently increasing electrical power output over a non-ventilated BIPV collector. However, the change in output depends heavily on the mode of operation. When supplied with a constant inlet temperature approximating mains water temperature annual electrical output can be increased 4.6%. When the same collector is connected to a domestic hot water tank where inlet temperatures float with tank temperature, a decrease in electrical output of 1.2% results. On the other hand, water temperatures of nearly 60ºC are possible with this system, so examination of the total energy capture is required. Overall thermal energy capture for the DHW system approaches 1,372 kWh or 4,681 KBTU, much higher than the losses introduced by the DHW tank. The ability of the collector to provide hot water for space heating or domestic use at little electrical penalty, or heat rejection for space cooling, makes a strong case for its implementation.

Natural Ventilation

Natural ventilation studies were performed in PHOENICS to determine the effect of building geometry on exterior pressure differentials and inform the size and location of operable windows. Local TMY2 weather data was evaluated to determine the direction of prevailing breezes. Figure 14 below shows a wind direction analysis of the weather data.

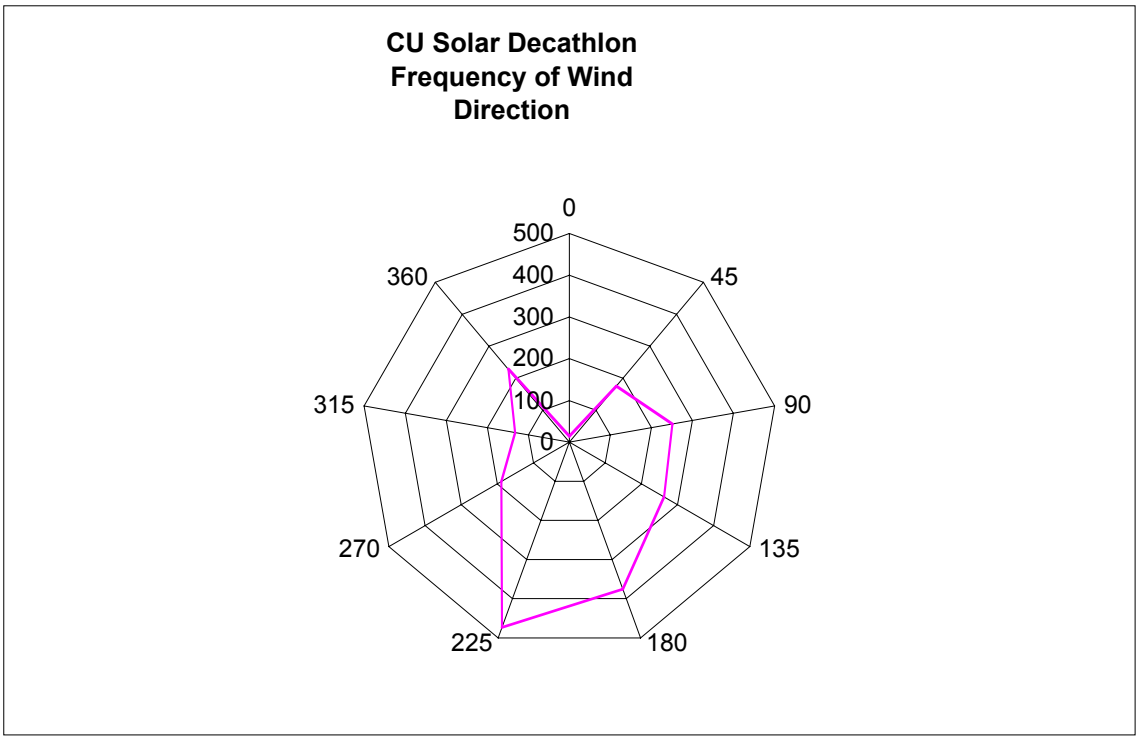

Figure 14: Prevailing wind direction during comfort conditions

This information was then used to construct a CFD model of the CU home. Using the prevailing wind direction of 225° from the analysis above and an average wind speed of 3m/s obtained form a similar analysis, simulations were constructed and results examined to find areas around the house suitable for locating windows. Figure 15 shows the results of one such simulation. Examination of this and similar plots resulted in the placement of operable windows on the

southwest corner of the building and at the clerestory area on the northeast corner of the building where no operable windows existed previously.

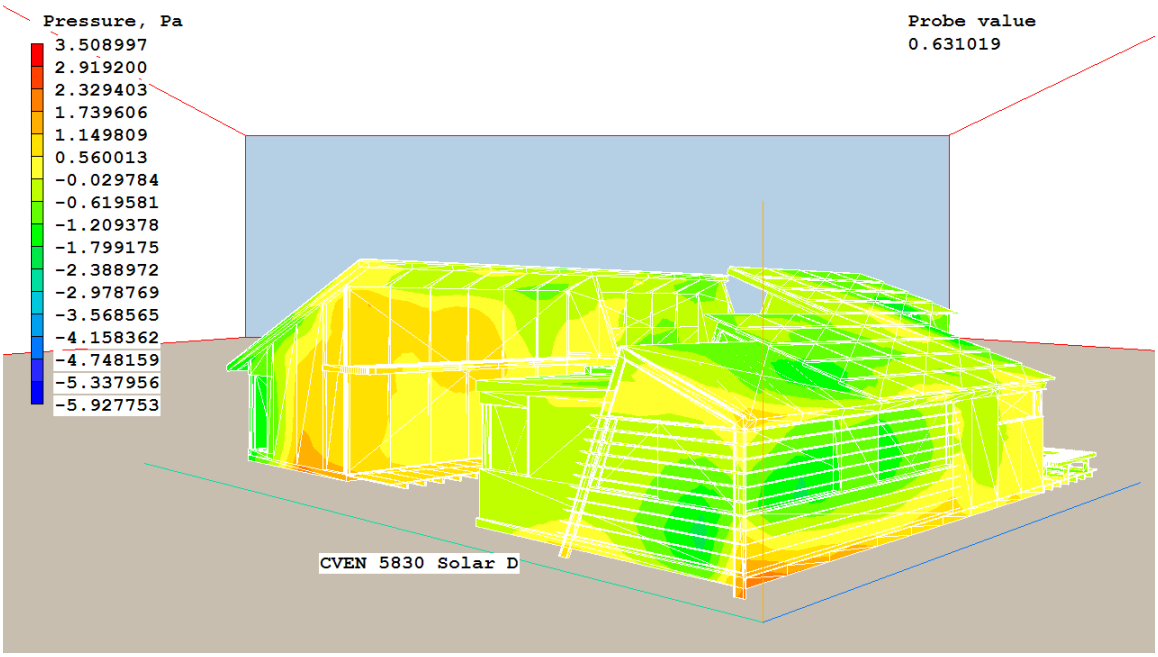

Figure 15: Pressure contours on CU building surfaces

Lighting

Initially, the lighting scheme (i.e. indirect, direct, and/or semi-direct lighting) was decided for each room of the house. Preliminary lighting analyses for each space were conducted using a Lumen Method spreadsheet, in order to determine an approximate number of required lumens, based upon the type of lighting. Next, appropriate light fixtures were selected to achieve the desired illuminance values. After each option of lighting type and placement was developed, AGI 32 was used to determine illuminance levels provided by the lighting fixtures at specific points within the 3D model of the house. Several different iterations were then run to help determine the correct quantity and placement of fixtures to meet the foot-candle requirements of the competition and to achieve desired aesthetics for the particular spaces. Figure 16 shows an AGI32 electric lighting rendering of one of the kitchen design iterations.

Figure 16: Kitchen electric lighting rendering, with an open-grid ceiling option

AGI 32 utilizes a full 3D modeling environment for the design and manipulation of the objects that interact with lighting. The 3D model of the house can be created using tools with in AGI or from imported AutoCAD 3D files. Light fixtures are simulated using photometric files of the specific fixture provided by the manufacturer. Another benefit of the software is that it allows for texture and color to be added to surfaces. As calculations are performed to determine light levels in the spaces, a rendering of the environment is also created. These renderings give the interior design teams an opportunity to view the materials selected in a more realistic environment.

Additionally, daylighting calculations were performed with AGI32 as well. Key locations within the space were monitored at different times of day and times of year, to minimize glare problems and ensure adequate daylight delivery during important hours of the day. Figure 17 shows one such daylight rendering in the bedroom loft area on a September afternoon.

Figure 17: AGI32 daylighting rendering of the bedroom loft, 1pm, September

PROJECTED PERFORMANCE OF COMPLETE HOUSE DESIGN ON AN ANNUAL BASIS

Modeling Approach

Annual system performance of the CU home was evaluated using Energy+ and TRNSYS for three locations and compared to the energy use of a similar home built according to the Building America Benchmark (BABM). TRNSYS was chosen because of its ability to model complex systems that cannot be accurately modeled by other whole-building energy simulations tools.

The BABM building was modeled in Energy+ using published BABM guidelines obtained from the EERE website. Values for building construction, miscellaneous plug loads, lighting type and HVAC system efficiency are based on the size, location and features of the CU prototype home. Typical domestic hot water and appliance use schedules were applied according to the benchmark specifications. Annual simulations were performed to determine heating, cooling and electric loads.

A separate Energy+ model was created representing the construction of the 2,100 ft^2 CU prototype home. . The CU home includes energy efficiency measures such as high-performance walls and windows, fluorescent lighting, automated natural ventilation, and a novel HVAC system. Schedules were assumed to be the same for both homes, however, more efficient appliances were chosen for the competition home. Energy+ was used to generate heating, cooling, lighting and miscellaneous electric loads only. Loads were then input into a TRNSYS model where they were used to simulate the performance of the HVAC and PV/T. Previous modeling of each component discussed above informed the size and parameters to be used in the prototype home and TRNSYS simulation.

Several key parameters defining the construction of the BABM home and important differences between it and the CU prototype are summarized in the table below:

Table 3: Modeling differences between benchmark and prototype home

	BABM House	**CU Prototype**
Window Area/Floor Area	18% based on BABM equation for detached single family home	18% based on parametric window study
Wall Construction	R-17.2 based on Paragraph 502.2 of the 2003 IECC	R-42 typical SIP wall construction
Window Characteristics	U=0.39 SHGC-0.32 based on HERS methodology	U=0.14 SHGC=0.47 based on parametric window study and manufacturer data
Miscellaneous Electric Loads	Load and schedules based on BABM Analysis Spreadsheet	Load based on manufacturer data for energy use.
Electric Lighting	Indoor and Outdoor loads and incandescent percentage based on floor area per BABM	As designed
Natural ventilation	33% probability of window opening 3 days per week	50% probability of window opening
Sunspace	Not allowed by BABM	As designed
HVAC (cooling)	Air-to-air split system with	Water-to-water based on

	HSPF=6.8	manufacturer data
HVAC (heating)	Air-to-air split system with HSPF=6.8	Water-to-water based on manufacturer date
Heating & Cooling Setpoints	21.6°C and 24.4°C	21.6°C and 24.4°C
Shading	Not allowed by BABM	As designed
Attic	None	None
Crawlspace	Yes	Yes

One important difference between our simulated benchmark building performance and that of a "true" BABM is the periods of HVAC operation. The BABM identifies the availability of heating and cooling based on monthly average ambient temperature. For our location in Boulder, CO, the BABM would dictate that cooling is available only during the months of July and August. (The presence in the TMY2 dataset of three cold days in early June exerts exceptional influence over the monthly average temperature.) The simulation of both the BABM building and our prototype building indicate that indoor temperature would be unacceptably warm for most of the month of June. We believe that it is more representative to enable cooling in June and have performed our analysis accordingly.

TRNSYS Model Definition

A TRNSYS 16 model of the CU home was constructed to model the combined performance of the HAVC and solar system components. The simulation was modeled as closely as possible to the proposed system except where TRNSYS did not have an equivalent component and/or simplifying assumptions were made for the analysis. No components used in the model were custom written for the evaluation. A schematic of the system, minus control components, is shown below in Figure 18:

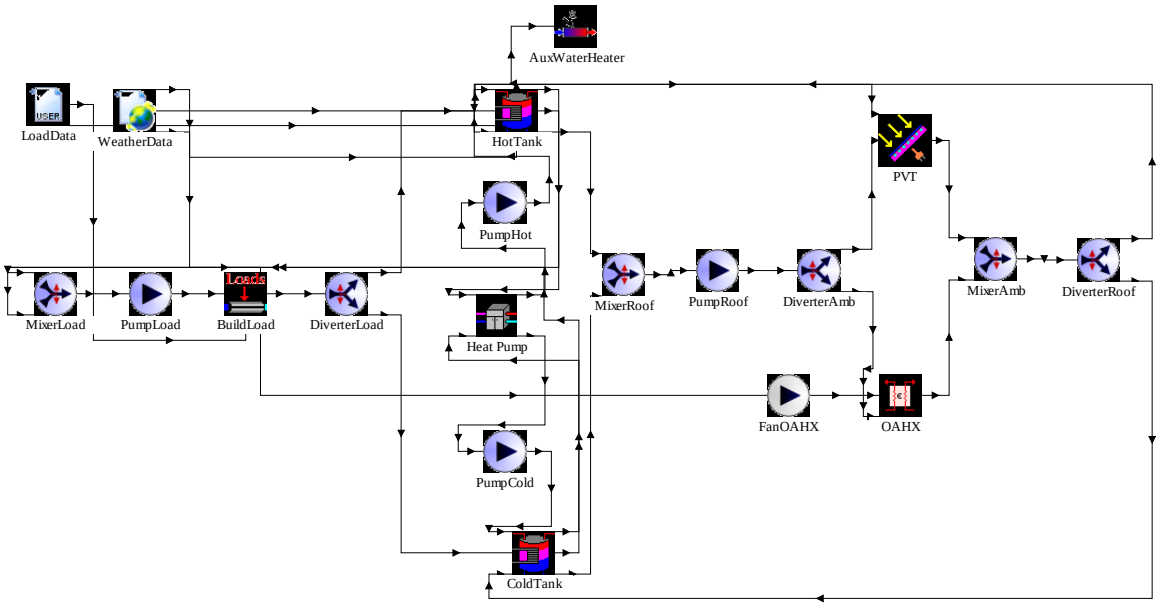

Figure 18: TRNSYS System Schematic

The cold water/ice storage tank was simulated by a stratified water tank allowed to drop below the freezing point of water. In operation, the temperature will remain at 0C as energy continues to be extracted by the heat-pump. The simplification was necessary to account for the additional

latent energy available from water as it freezes in lieu of an ice storage model. Though not entirely representative of the actual system operation, this simplification is conservative and is expected to under-predict the overall performance of the system. Initial simulations show that the tank temperature drops below freezing only 538 hours of the year, representing only 6% of the simulation duration and justifying the simplification made to the model.

The construction of the CU home's PV/T collector, shown in Figure 19, differs from the typical geometry in that the thermal tubing does not make physical contact with the PV modules. Rather, the thermal absorber is separated by a small air gap. The PV/T model that most closely resembles our collector, component Type 560, assumes that the fin-tube absorber is bonded to the PV substrate with a fixed thermal resistance. The system was modeled by using an effective thermal resistance of 0.176 m^2K/W (1.0 hr $ft^2°F/Btu$). Strictly speaking, the effective resistance of our air gap will vary due to the influence of surface temperatures on the natural convection. The chosen value is conservative. Other important collector parameters were derived from earlier MATLAB and PHOENICS models discussed previously.

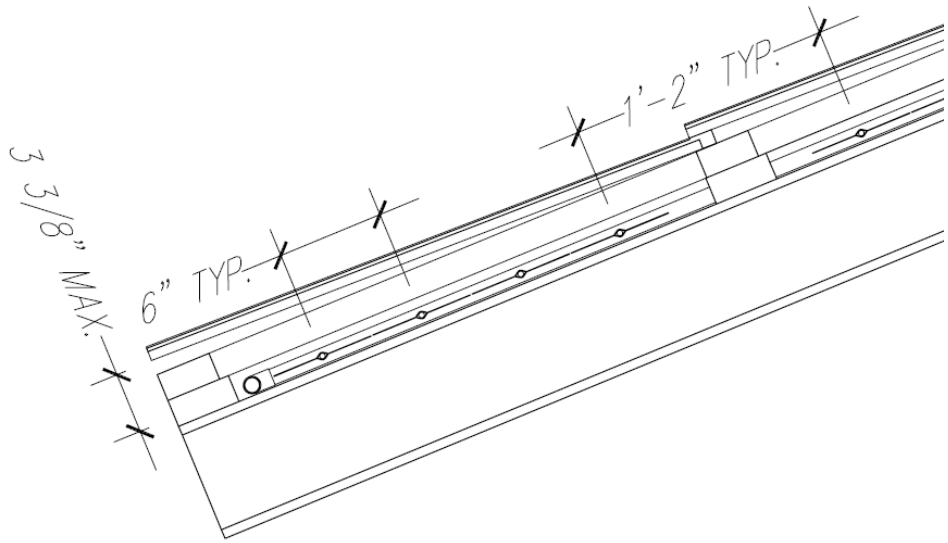

Figure 19: BIPV/T Collector

The heat-pump to be used in the prototype home is a new model that has yet to be release to the market. This unit is designed with two separate hot water loops at the condenser: warm water for space heating and hot water for domestic use. Unlike previous models that used a desuperheater, this model will allow full condenser heat for water heating. Exact performance data for the heat-pump was unavailable at the time of modeling. Our analysis was performed using the performance map of the product line that preceded the new produce. Actual performance is expected to be higher than the simulated performance. Unfortunately, no performance data were available at the highest inlet water temperatures expected for DHW heating.

The TRNSYS water-to-water heat pump model assumes a single condenser. Given the lack of performance data at high temperatures and uncertainty about the detailed control logic for switching between space and domestic water heating modes, we elected to significantly simplify the water heating model. To account for the electricity required by the heat-pump for domestic hot water, we assumed a fixed COP of 3.0 based on existing performance map data for entering

cold and hot water temperatures of 10°C and 50°C, respectively. Within the model, an inline heater with a COP of 3.0 was added to the system model to heat the water to the necessary temperature. (Note that model accurately accounts for the fact that the mains water is preheated by a heat exchanger in the hot tank before being delivered to a small DHW tank.)

Control logic implemented in TRNSYS operates the system to satisfy the building loads calculated by Energy+. In heating mode, the hot tank is maintained at a setpoint temperature by the heat pump. When PV/T collector temperate exceeds the cold tank temperature by a fixed differential, water is circulated to the collector to warm the cold tank. Hot tank temperature is allowed to float during heating mode and is not specifically controlled. In cooling mode, the logic is reversed and the cold tank is maintained at a setpoint temperature. Water is circulated to the roof when outdoor temperature is lower than the hot tank temperature and circulated to the outdoor heat exchanger when PV/T is not available for cooling.

Other operating modes continue to be explored, but have not yet been implemented in the system model. Controls not yet simulated include direct-to-load control of the heat pump, domestic hot water production from the PV/T, and variable storage tank setpoint temperatures. Current controls analysis includes the development of a strategy to optimally distribute heat from the PV/T system between the hot and cold tanks. In its basic operation, the PV/T heats the cold tank in winter and cools the hot tank in summer. However, in winter, the PV/T system is large enough that it could heat the cold tank above the temperature of the hot tank, with excess energy available to provide direct heating of the hot tank like a traditional solar water heating system. We are also working to optimize the proper setpoint of the hot tank in summer to recognize the competing needs for a high temperature to heat domestic hot water and a lower temperature to improve heat pump efficiency.

Case Descriptions

The following cases were examined to determine the performance differences between the BABM benchmark home and the CU prototype.

Case 1: BABM

Case 1 simulates the performance of a BABM building in Denver, CO. Plug loads, occupant schedules, lighting types and building construction are proscribed by the BABM spreadsheet. Case 1 simulation results form the basis of comparison for energy efficiency improvements.

Case 2: Prototype House with Building Integrated PV/T

Case 2 simulates the performance of the prototype house, which includes energy efficiency improvements and renewable energy systems. Results show the impact of energy efficiency measures on total energy use and production. System performance of the prototype house was evaluated in Phoenix, AZ, Denver, CO, and Sterling, VA to evaluate location specific performance.

Case 3: Prototype House with Building Integrated PV

Case 3 is similar to case 2 except that the thermal component of the PV/T collector has been disabled. Differences in energy use and production over case 2 highlight the role of active heat recovery in reducing the installed cell temperatures typical of BIPV. Case 3 is only simulated in Denver, CO.

Results

Case 1: BABM

Benchmark house simulation results show a maximum energy use in January of 8,382MJ, a minimum of 4,017MJ in September and annual energy use of 70,632MJ. High energy use in winter months can be attributed to the heating dominated climate of Denver, CO and the relative inefficiency of an air-to-air heat-pump with low source-side temperatures. Note that cooling energy is required in June per the modification to the benchmark assumption discussed previously. Also note that water heating loads vary as expected due to the variation in mains temperature throughout the seasons. Figure 20 shows the results of the BABM simulation by end-use.

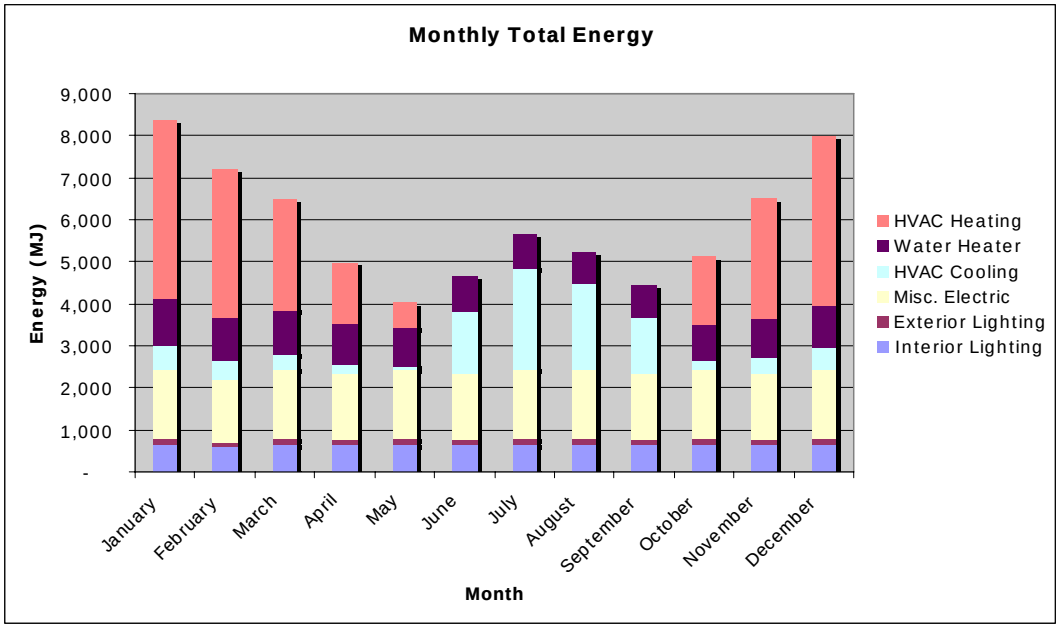

Figure 20: Monthly total electricity use for BABM building in Denver, CO

Case 2: Prototype House with Building Integrated PV/T

Denver, CO

The prototype results show the drastic impact of energy efficiency measures and site generation on overall energy use and annual energy balance. Peak loads still appear in the winter months, but the curve is flattened with additional peaks occurring in the summer cooling season. Peak electricity use occurs in January at 2,814MJ nearly 34% the peak load of the benchmark. October is the month with the lowest electricity use at 2,087MJ. Annual energy use is 28,985MJ, or 41% of the benchmark energy usage. Note the relatively low heating and cooling energy required for space conditioning in Figure 21 due to the higher efficiency of the water-to-water heat-pump and coupled thermal storage. Note also the decrease in lighting loads as function of an increased percentage of fluorescent lighting.

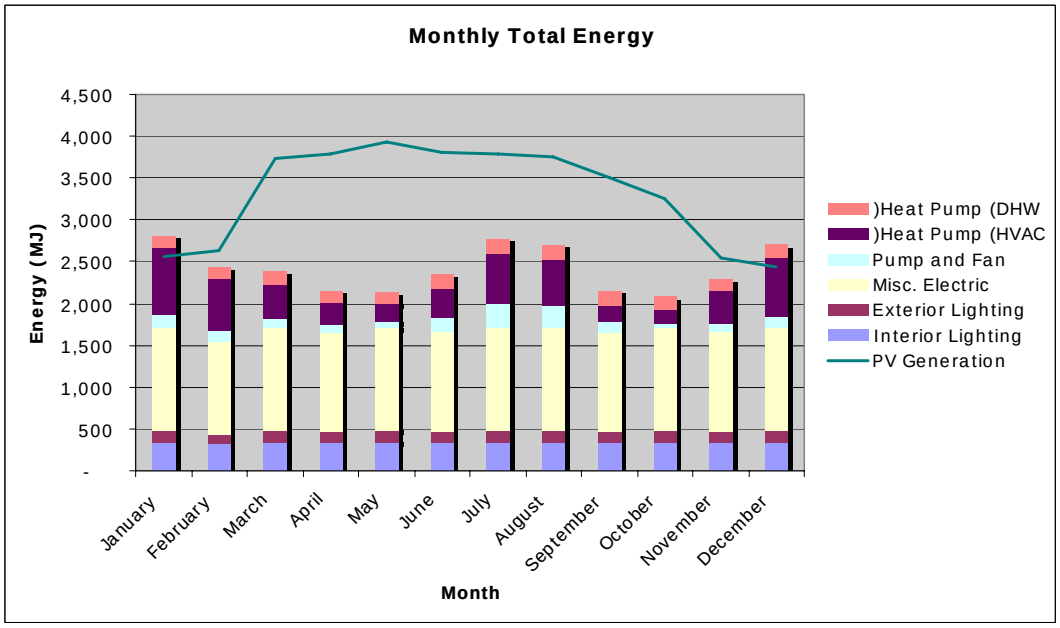

Figure 21: Monthly total electricity use for prototype building in Denver, CO

Total solar energy capture and energy rejection through the PV/T collector relative to heating and cooling loads is shown in Figure 22. Note that total solar electricity production is greater than the total electrical load of the building by nearly 25%; the prototype house is a net energy producer. Solar energy captured and rejected through the PV/T system is nearly as great as the building heating and cooling requirements, contributing to the overall efficiency of the HVAC system by reducing the amount of time the heat-pump runs. Total PV electricity production is 39,725MJ and total heat production from the PV/T is 14,908MJ.

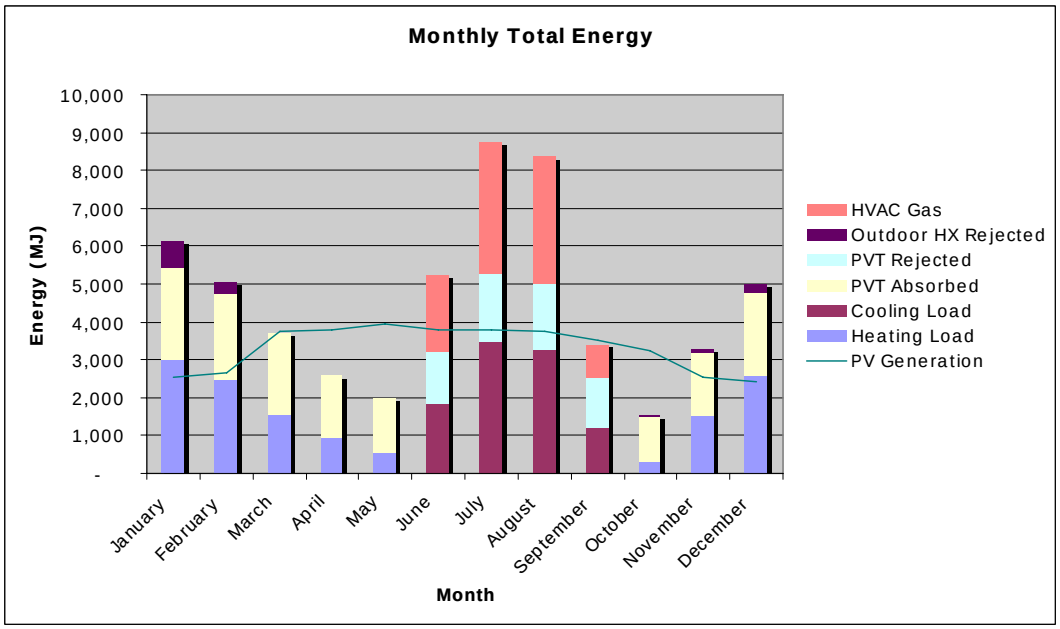

Figure 22: Total solar energy production and outdoor heat exchanger energy capture in Denver, CO

To examine the impact to of system controls on the energy use of the house, one additional simulation was performed for Denver. In this simulation, the hot tank's setpoint temperature was increased by 5°C to 50°C. The resulting change in annual energy use is not insignificant. Total annual energy use rises to 30,376, representing an increase of 4.8%. While energy requirements for hot water fall by a margin of 26%, heat-pump and fan energy increase by a margin of 34%. Despite the increase in energy use, the simulation shows that the home is still a net energy producer.

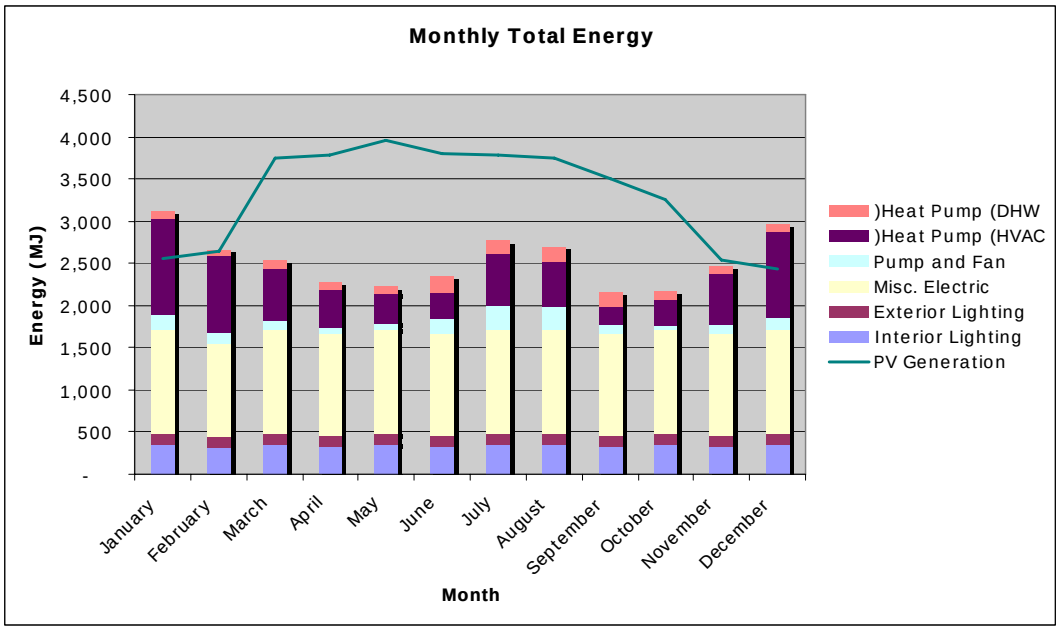

Figure 23: Total solar energy production and outdoor heat exchanger energy capture in Denver, CO with hot tank setpoint of 50°C

Phoenix, AZ

Results from the Phoenix simulation can be seen in Figure 24. Total energy peaks during summer months as expected due to the cooling dominated climate; heat-pump cooling energy is approximately 2.4 times that of Denver. Energy requirements in July total 5,234MJ and total 37,531MJ annually. Net electricity production reaches 44,417MJ annually, resulting in net electricity production.

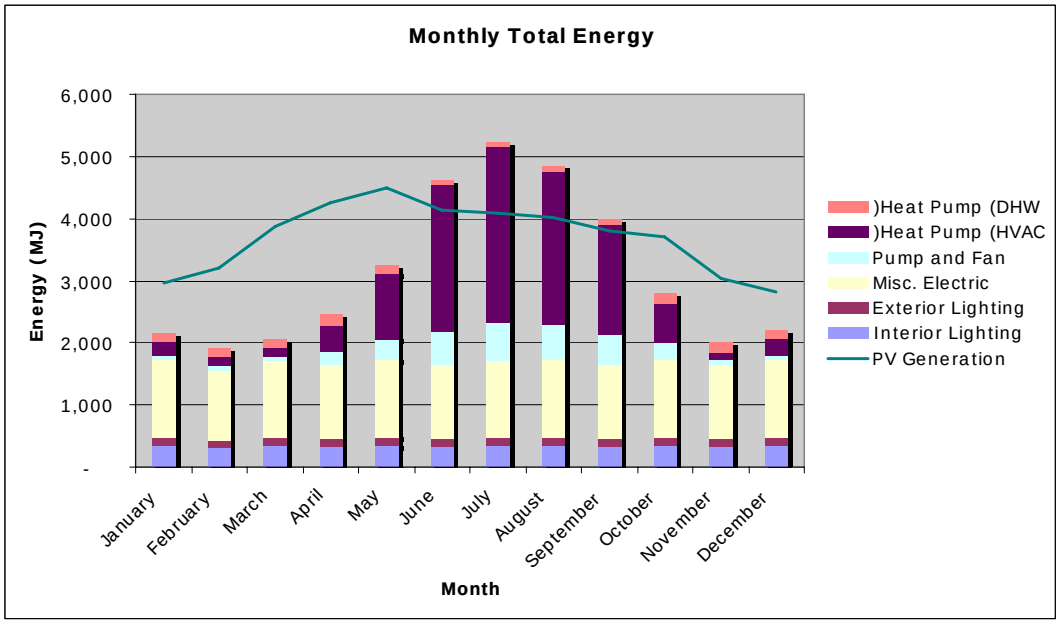

Figure 24: Monthly total electricity use for prototype building in Phoenix, AZ

Sterling, VA

The energy use profile for the prototype house in Virginia shows similar trends when compared to Denver. Both locations show nearly equal heating and cooling peaks with the lowest energy use occurring during the swing seasons. Peak electricity use occurs in July at 3,774MJ, while October is the month with the lowest electricity use at 2,044MJ. Annual energy use for Sterling is 33,269MJ and total electrical production is 33,857MJ. The same house in Virginia is still a net energy producer albeit at a much smaller margin than either Denver or Phoenix. This can be attributed to the relatively high HVAC and pump energy use and lower overall electricity production from PV due to a higher incidence of cloud cover.

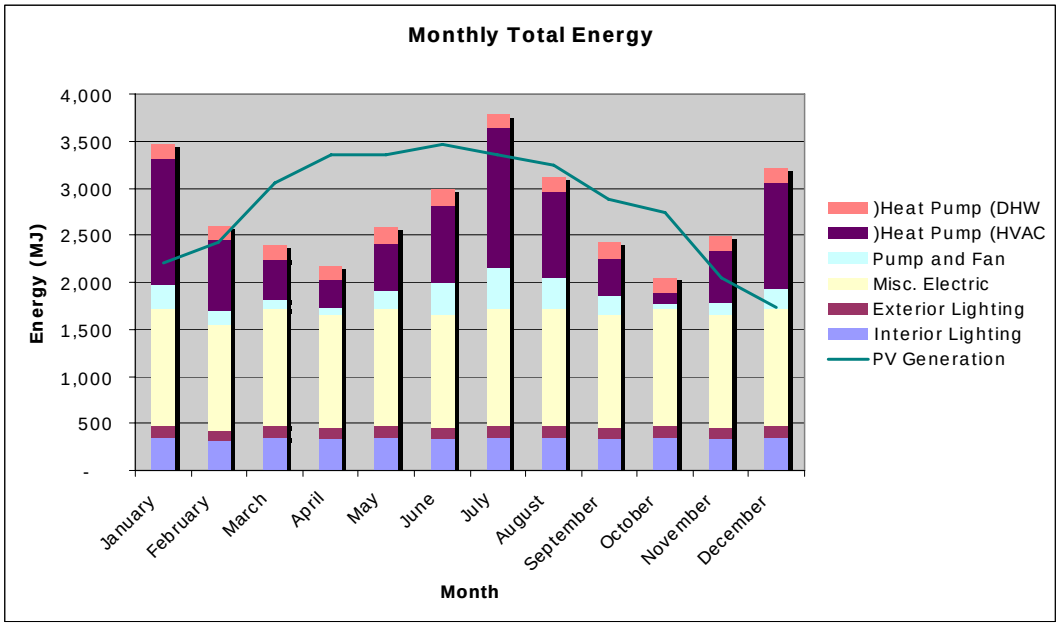

Figure 25: Monthly total electricity use for prototype building in Sterling, VA

Case 3: Prototype House with Building Integrated PV

Figure 26 shows the results of the prototype house in Denver, CO with the thermal component of the PV/T collector disabled. Total PV energy production drops to 39,102MJ, a loss of 1.5% of the energy production over the previous case. Consequently, total annual energy use increases to 29,871MJ, a difference of 3.1%. PV production relative to Case 2 is smallest in February with a 3.7% decrease in output. The increase in annual energy can be attributed entirely to the additional energy required to power the outdoor heat exchanger fans and heat-pump to satisfy building loads. Gains in PV/T efficiency through different implementations would very likely decrease fan and heat-pump energy requirements further.

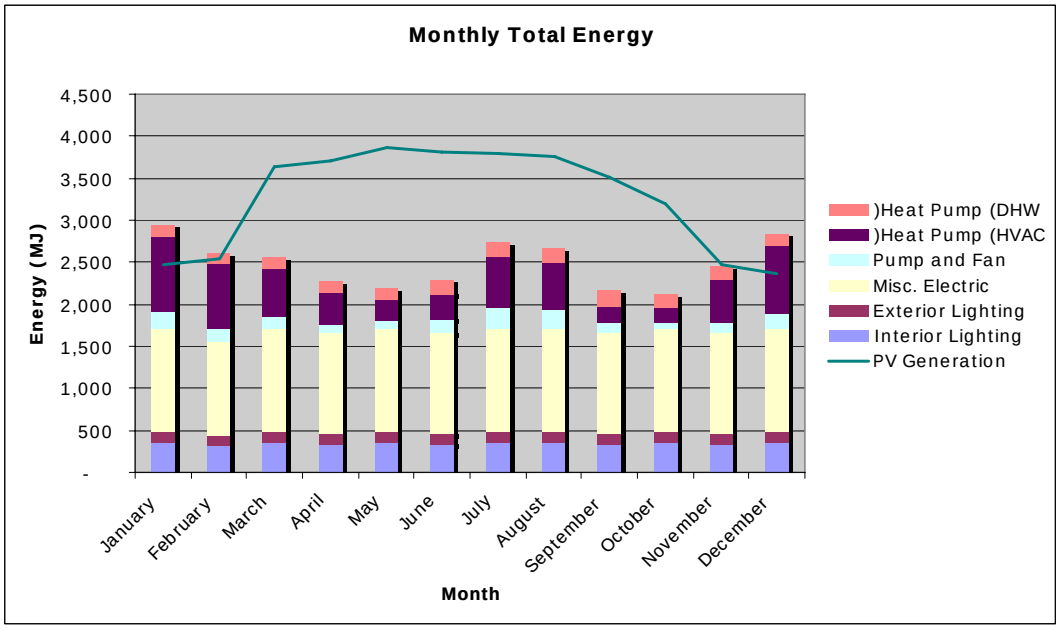

Figure 26: Monthly total electricity use for prototype building in Denver, CO without PV/T

Conclusions

The CU prototype home shows significant energy savings when compared to the Building America Benchmark home. Energy efficiency measures implemented in the prototype home result in a reduction in electricity use by 59% over the benchmark. The PV/T system is more than capable of providing enough electrical and thermal energy to satisfy all energy requirements, resulting in a home that is a net energy producer in all three test climates. Optimization of system controls will likely have a significant impact on total energy use as indicated by the adverse effects of an increased setpoint temperature. The modest impact of the PV/T system over a standard BIPV installation on total energy use must be considered as an alternative to additional PV, but must be carefully evaluated for each climate.